Processing–Property Interactions in Poly(vinylidene Fluoride). II. Morphology and Property Characterization of Extruded Films

B. KHOMAMI and A. J. McHUGH, *Department of Chemical Engineering, University of Illinois, Urbana, Illinois 61801*

Synopsis

The effects of flow history, processing temperature, and exit draw ratio have been studied for a poly(vinylidene fluoride) resin. Quantification of the stress fields and flow kinematics were described in Part I while, in this publication, attention has been addressed to the evaluation of film properties. Hot-stage and differential scanning colorimetry (DSC) analyses were used to characterize the thermal behavior; polarized light optical microscopy and electron microscopy were used to characterize the morphology; Fourier transform infrared (FTIR) and wide-angle x-ray scattering (WAXS) were used to evaluate crystal structure; and mechanical testing was used to evaluate tensile properties. Extensional melt stresses on the order of 1.4×10^6 dyne/cm^2 were necessary to induce row-nucleated crystallization in undrawn samples, and in all cases, preorientation of the melt by extensional flow enhanced the efficiency of the $\alpha \rightarrow \beta$ transformation with drawing. The various transformations on drawing were as follows: unoriented α to oriented superheatable α phase for draw ratio (DR) < 5; transformation from α to β phase for $5 < \mathrm{DR} \leq 25$; transformation to more highly oriented α and β phases, DR > 25.

INTRODUCTION

Poly(vinylidene fluoride) (PVF_2) is an important thermoplastic material valued both for its piezo- and pyroelectric properties[1,2] and also because of its polymorphism which results in an unusual range of processing–property interactions. At least four known crystal structures can occur [α (form II), β (form I), γ (form III), and δ or α_p (form IV_p)], and a possible fifth crystalline modification has recently been suggested by Lovinger.[3] Since essentially no studies of the effects of melt flow history have been reported for this material, we have focused attention on this aspect. In a companion paper (Part I), results of our analysis of the melt extensional flow history in an impinging channels die geometry were presented. In this report, attention will be focused on the properties of both as-extruded and drawn films produced in this geometry. Since several of the earlier studies on the structural aspects of PVF_2 films are a focal point for comparison, we begin with a brief review of these.

BACKGROUND

The most common polymorph of PVF_2 is the α form (form II) which is produced by cooling from the melt. Based on x-ray analysis by Bachmann and

Journal of Applied Polymer Science, Vol. 36, 877–889 (1988)
 CCC 0021-8995/88/040877-13$04.00

Lando,[4] the α-unit cell is orthorhombic, having dimensions a = 4.96 Å, b = 9.64 Å, and c = 4.62 Å, and contains two chains. The configuration of the α phase, as suggested by Hasegawa et al.[5,6] is a distorted TGTG′ with T = 170° and G = 45°. In this polymorph, chain dipoles oppose each other in packing rendering this form nonpolar. The β phase (the piezoelectric and pyroelectric phase) is obtained by mechanical deformation of melt-crystallized films (T $\leq$ 130°C). Crystallization of the β phase from the melt has been uncertain until the recent success by Lovinger,[7] who obtained it by epitaxial melt solidification on the (001) surface of freshly cleared KBr. Gal' Perin et al.[8] have shown that the unit cell of the β phase contains two chains in orthorhombic symmetry with lattice constants a = 8.45Å, b = 4.88 Å, and c = 2.55 Å; however, Lando et al.[9] assigned the cell to be pseudohexagonal with slightly different a and b dimensions. The γ phase of PVF_2 can be obtained by crystallization from the melt at high pressure as well as by crystallization from certain solutions. Based on electron diffraction patterns from single crystals, Lovinger[10] suggested that, in this case, the unit cell is monoclinic with lattice constants a = 4.96 Å, b = 9.67 Å, c = 9.20 Å, and β = 93°. The δ phase of PVF_2 is formed by poling the α phase at high electric fields, therefore, it is also known as a α_p phase. According to Bachmann et al.,[11] the unit cell is orthorhombic with a = 4.96 Å, b = 9.64 Å, and c = 4.62 Å. Although the lattice parameters are identical to those of the α phase, the difference lies in the interchain packing. The ab projection of the δ phase exhibits a TGTG′ conformation with the dipole vector pointing in the same direction, whereas the ab projection of the α phase shows dipoles in opposite directions.

Transformation of melt-crystallized α-phase to β-phase crystals and its extent has been shown to be a very strong function of draw temperature.[12-14] At low draw temperature (i.e., 80°C to 100°C) transformation of α phase to oriented β phase occurs readily at draw ratios up to 400% engineering strain. At high temperatures, oriented α phase is obtained up to these draw ratios, and it is only by drawing the material further that the β form becomes the dominant phase.[13,15] Similar behavior for PVF_2 rods, but occurring at lower draw ratios (i.e., 200%), was reported by Richardson et al.,[16] based on x-ray diffraction. Matsushige et al.[14] demonstrated that a heterogenous stress distribution in the sample played a critically important role in the crystal transformation phenomena. Using x-ray diffraction, they observed the transformation in films which were drawn at temperatures below about 130°C. Initiation of the phase transformation was detected at the deformation stage where necking began.

Most investigations of the α- to β-phase transformation have used x-ray diffraction and infrared spectroscopy. Fewer studies of the stress-induced morphological changes have been reported.[15,17] A recent study[18] of the morphological aspects of α- to β-phase transformation during deformation of both thin (1000 Å) and thick (1 mm) films has demonstrated that transformation occurs at the point where fibrils are formed during deformation.

The crystal transformation of α to β phase of PVF_2 during extrusion has been limited to solid-state extrusion or solid-state coextrusion.[19-21] In their work Shimada et al.[19] performed solid-state extrusion of PVF_2 in conical and

slit dies to an extrusion draw ratio of 8 where high chain orientation of the crystallizable phase in the extrusion direction was observed. Their films exhibited strain hardening corresponding to a rapid decrease in extrusion rate or a rapid increase in the apparent elongational viscosity with draw ratio to a maximum draw ratio of 7. An increase in the tensile modulus from 1.2 Gpa to 3.2 Gpa was observed as the draw ratio was increased from 4 to 7. Mead et al.[20] in their solid-state coextrusion of high density polyethylene (HDPE) and PVF_2, demonstrated the crystal transformation from α to β phase through differential scanning colorimetry (DSC) and infrared spectroscopy. They produced a superheatable β phase with a reported melting point of 171°C at a draw ratio of ~ 5.3 (their maximum draw ratio).

It is not clear from these studies whether, or how much, preorientation in the melt state may influence the efficiency of the α to β transformation, especially at higher draw temperatures (e.g., ~ 130°C). Likewise, it is apparent that relatively little is known regarding the effects of melt flow history and orientation on the crystallization process itself, either with regard to morphology or crystal structure development. For these reasons we have focused attention on these aspects of the problem. In particular we have been interested in evaluating the effects of a quantifiable extensional flow on the morphology and properties of as-extruded and drawn films. Complete details on the stress and flow field analysis, as well as details on the die flow geometry, operating conditions, and properties of the Solef resin used in our studies are given in Part I. For comparison purposes, we have also carried out a number of extrusion runs using the standard slit-flow die also described in Part I. A variety of techniques were used to characterize the properties of the films produced in these geometries, the details of which are presented and discussed in the following sections.

CHARACTERIZATION

Optical microscopy was carried out on a Nikon 104 polarizing microscope, fitted with a video recording system and thermal behavior was also monitored using a standard hot stage heating attachment. More detailed thermal analyses were carried out on a Perkin-Elmer DSC-4 calorimeter interfaced to a System 714 thermal analysis controller and model 3600 data station. Melting endotherms were generally obtained at heating rates of 5 and 10°C/min, and, in a number of instances, samples were allowed to crystallize followed by remelting. The effect of heating rate on peak positions was tested over the range from 2.5°C/min to 10°C min. In all cases shifts were on the order of or less than 0.1°C.

Infrared spectra were obtained using a Nicolet system (7000 series) Fourier transform infrared (FTIR) apparatus following standard procedures. X-ray diffraction patterns were obtained on a Raguka (rotating camera) device equipped with a microcomputer. Both flat face (i.e., a–b direction) and draw direction (i.e., c direction) scans were taken and rocking curve analyses were used to determine crystallite c-axis distribution. Scanning and transmission microscopy were carried out following standard preparation procedures. Fi-

nally, the Young's modulus was measured on an MTS model 820 tester. The modulus was determined from the tangent to the stress–strain curve at 0.1% strain. The strain rate was 1.67×10^{-2} s^{-1}.

RESULTS AND DISCUSSION

Thermal Behavior and Morphology

The overall melting point, as determined by the disappearance of birefringence on the optical hot stage, gives an impression of the general trends with processing conditions. As shown in Table I one finds that for a fixed flow rate and extrusion temperature, melting points increase with decreasing take-up draw ratio (DR) (defined as the ratio of die exit to final film cross-sectional areas), ranging from 179°C for the as-quenched samples (i.e., water or air cooled) to 174°C for the high draw ratios. As will be shown, this trend reflects the presence of an increased fraction of the lower melting, oriented β phase with increasing draw. The lack of substantial difference between the first and second melting scans reflects the fact that the hot-stage measurement does not discern the presence of separate melting species. As will be shown shortly, DSC scans show the presence of overlapping peaks in several of these samples corresponding to the coexistence of α and β phases.

As shown in Figure 1, optical micrographs clearly exhibit the presence of row-nucleated structures in the draw direction. This behavior is what one would expect for a drawn film. Likewise, as seen in Figure 2, the overall degree of crystallinity (determined by the light area of the micrograph) monotonically increases with draw ratio, plateauing around 40 to 60%. A similar pattern was reported by Mead et al.[20] for a solid-state, conventionally extruded Kynar resin at lower draw ratio. On the other hand, as seen in Figure 3, above a critical flow rate, row-nucleated structures can be induced by die extrusion alone (i.e., in the absence of a take-up draw) with this geometry. At lower flow rates, and, likewise, for films extruded in the slit-die system, the morphology consisted solely of connected spherulites. Thus, from our stress

TABLE I
Hot-Stage Melting Points

Extrusion temp (°C)	Draw ratio	T_m (1st scan) (°C)	T_m (2nd scan) (°C)
220	65	174	175
	17	175	175
	6	176	177
	0/quenched	179	180
210	50	174	175
	15	175	175
	4	176	177
	0/quenched	179	180
200	85	174	175
	24	174	175
	15	176	177
	0/quenched	179	180

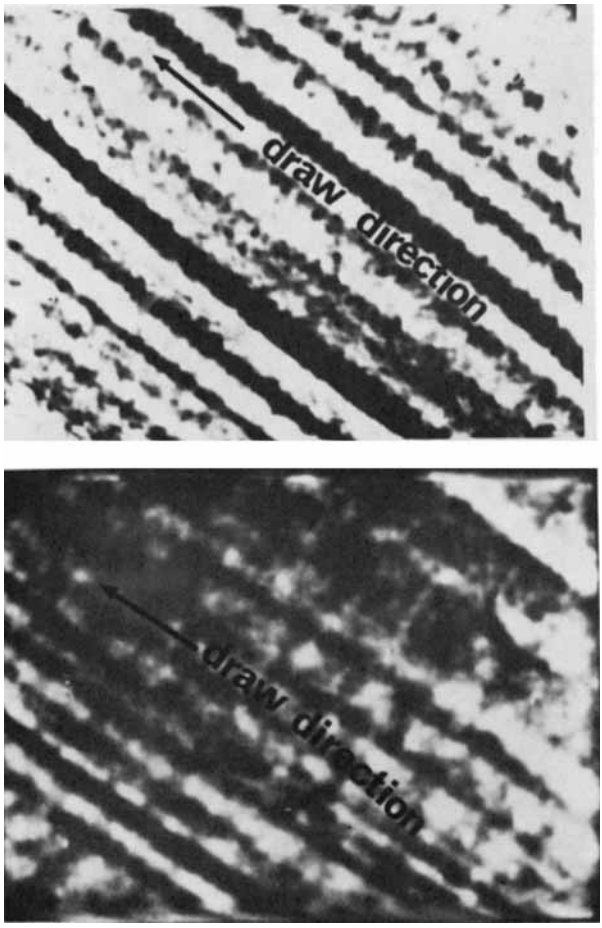

Fig. 1. Optical polarized light micrographs of drawn films. Top: draw ratio = 65; bottom: draw ratio = 15.

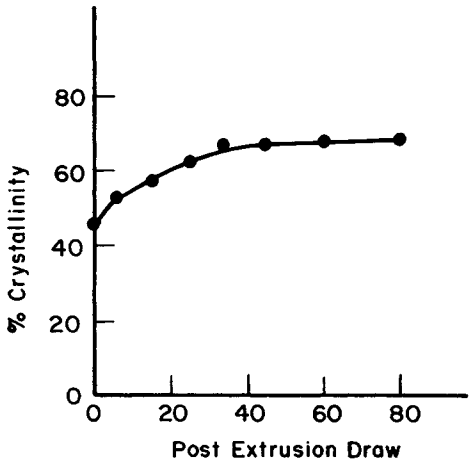

Fig. 2. Percent crystallinity as a function of draw ratio for films extruded at °C.

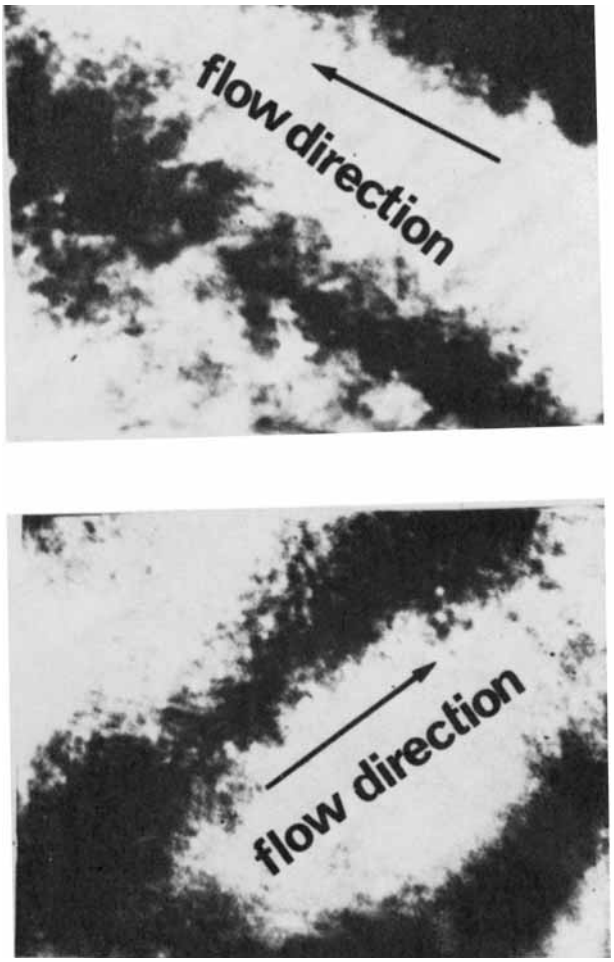

Fig. 3. Optical polarized light micrographs of undrawn films extruded at $T = 200°C$ and two-dimensional die flow rate $q = 0.01$ cm^2/s. Top: water-cooled; bottom: air cooled.

birefringence measurements (Part I), we conclude that normal stresses on the order of 1.4×10^6 dyne/cm^2 generated by the extensional die flow are necessary to induce row-nucleated crystallization in this system. As expected, in all cases, random, spherulitic structures resulted on recrystallization.

The effects of die flow rate on oriented structure formation were also exhibited in the DSC data. Figure 4 shows thermal profiles of two samples (water cooled) which were extruded at 210°C and the two-dimensional flow rates indicated. Both exhibit a broad peak at about 174°C with a range from 160° to 182°C. The increased superheatability of the film extruded at the higher flow rate, however, indicates the increased presence of more oriented crystals of the α phase. Thermal profiles of the undrawn, air-cooled samples also showed similar trends, however, superheatability was reduced by as much as 2°C due to relaxation of the melt during the slower crystallization. For the

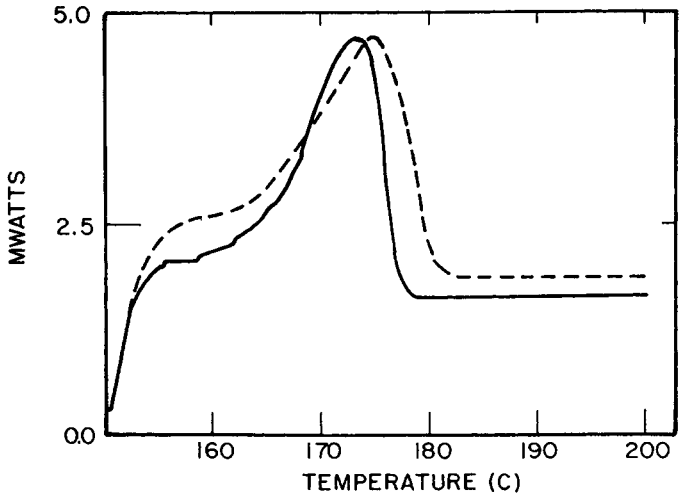

Fig. 4. DSC profiles of water-cooled film extruded at $T = 210°C$. (—) $q = 0.016$ cm^2/s; (---) $q = 0.03$ cm^2/s.

range of extrusion temperatures, 200°C < T < 220°C, the effects of temperature on the final thermal profile were much less pronounced than for the flow rate.

Several interesting effects of draw ratio on the thermal profile can be seen in Figure 5. Comparison of the profile for the sample having a draw ratio of 6 to those in Figure 4 indicates that, upon drawing, the melting range decreases and the peak shifts downward to 171°C with a shoulder at 173°C. Thus, the highly oriented material in the superheatable tail is being partially converted to the lower melting β phase as also suggested by the hot-stage data in Table I. The extent of transformation increases with draw ratio, and, at a value of 15, the profile exhibits two distinct peaks, one at 167°C corresponding to the β polymorph[20] and one at 173°C corresponding to the oriented α phase. Increasing the draw ratio to 65 does not alter the peak temperatures, however, the similarity in areas indicates, that, rather than inducing further $\alpha \rightarrow \beta$ transformation, the additional draw increases the amount of oriented α phase. This is consistent with other studies[14,20] which have established that at temperatures higher than 75°C the amount of crystal transformation will depend on the draw temperature (i.e., the β phase which forms under our draw conditions is being produced at a draw ratio of approximately 5 to 15, and, because of thermodynamic constraints, further crystal transformation does not occur as a result of further draw).

The profile for a draw ratio of 85 again shows two distinct peaks with similar magnitudes to those at 65. Comparison to Figure 2 suggests that the additional draw, rather than inducing either further crystallinity or additional phase transformation, is simply producing higher orientation in the α and β phases. This is indicated by the 1°C increase in melting temperature and peak range of the β polymorph and the 2°C increase in peak range of the α crystals. In all cases, melting and recrystallization resulted in a single-peaked profile ($T_m = 172°C$), indicating complete disappearance of the β phase and complete relaxation of orientation in the α phase. Finally, it should be noted

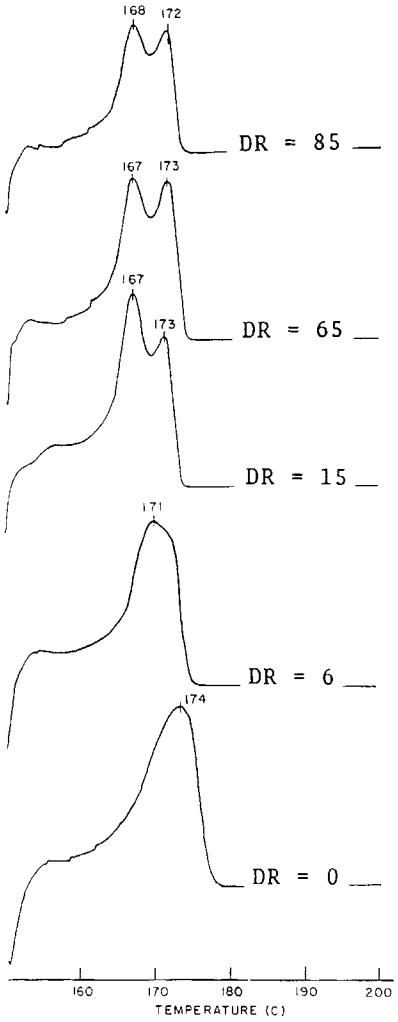

Fig. 5. DSC profiles of films extruded at a fixed flow rate (q = 0.03 cm^2/s) and temperature (T = 210°C) and indicated DR.

that under all conditions of draw, films extruded in the slit-die geometry exhibited only single broad-peaked endotherms (similar to the DR = 6 of Figure 5) and showed negligible β phase formation.

FTIR and X-ray

The assignment of α- and β-phase peaks in the DSC data is further substantiated by our FTIR and x-ray results.

Figure 6 shows several typical FTIR scans. The undrawn, water-cooled material exhibits peaks at 410, 490, 530, and 612 wavenumbers corresponding to the α phase.[6,14] For drawn films, in addition to the peaks at 410 and 612 for the α polymorph, new peaks appear at 442, 468, 475, and 509 wavenumbers corresponding to the β polymorph. Furthermore, as the draw ratio is increased from 5 to 25, the presence of the β polymorph becomes more

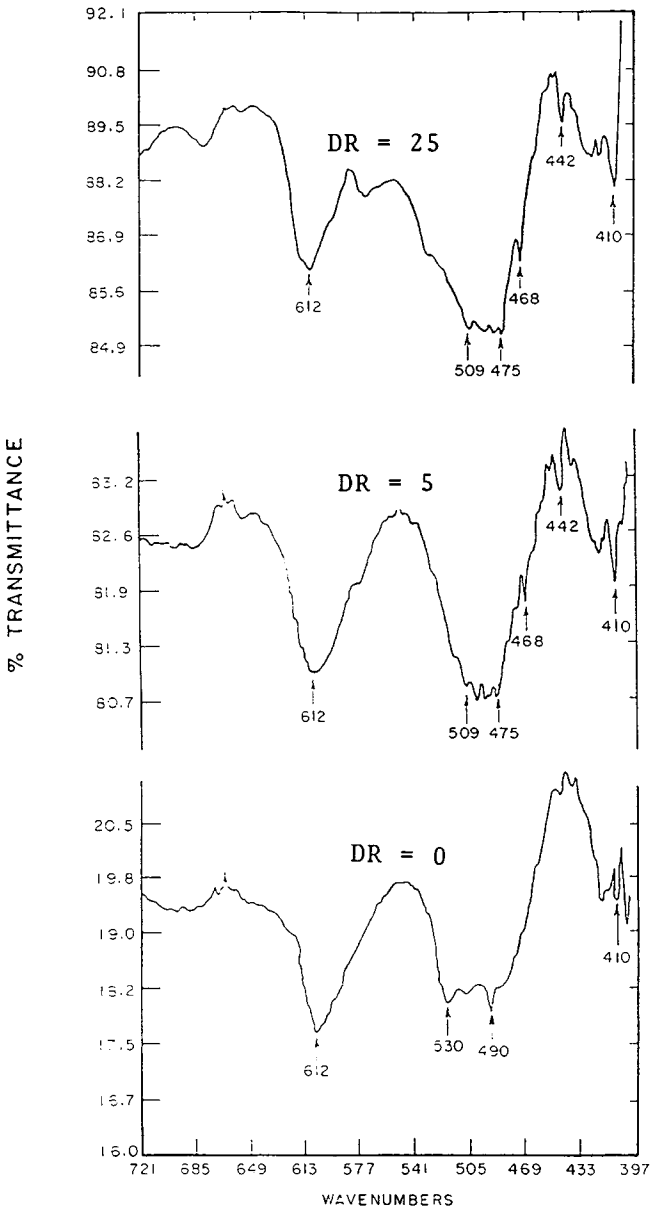

Fig. 6. FTIR scans of various films as a function of DR.

pronounced (the peaks at 509 and 468 are enlarged). Profiles of films with higher draw ratios (i.e., 25–85) resemble those for a draw ratio of 25, except for slight changes in the 612 peak.

Figure 7 shows flat-face x-ray scans for three separate films. The top two peak profiles are for draw ratios of 85 (middle) and 15 (top), while the bottom peak profile is for the undrawn water-cooled sample. The water-cooled material exhibits a broad peak at 18.3° followed by a peak at 20.5° corresponding, respectively, to the [020] and [110] plane of the α polymorph.[5,6,13] The

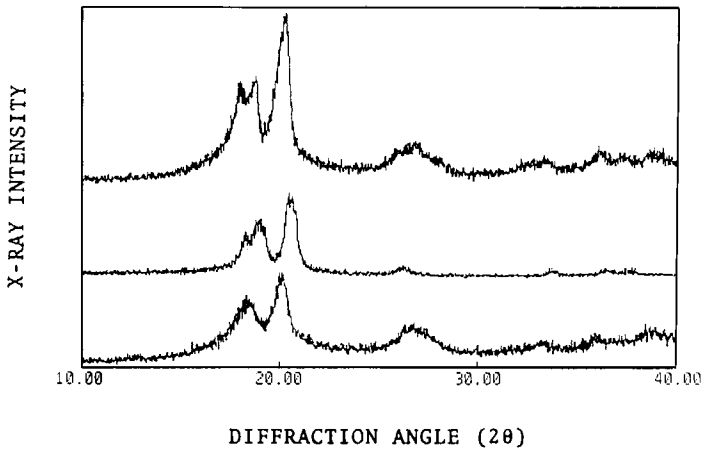

Fig. 7. Flat-face x-ray diffraction patterns of extruded films. $q = 0.016$ cm^2/s; $T = 200$°C. Top: draw ratio = 15; middle: draw ratio = 85; bottom: water cooled.

broadness of the first peak could be attributed to the presence of a very small [100] peak at 17.9°. The third peak at 26.7° corresponds to the [021] plane, however, the broadness is attributed to the presence of a smaller peak at 25.8° corresponding to the [120] plane of the α polymorph. The peaks at the higher diffraction angles are attributed to the [130], [200], [131], and [210] peaks of the α polymorph. With increased draw ratio (top peak profile) two distinct peaks, at 17.9° and 18.5° appear corresponding, respectively, to the [100] and [020] peaks of the α polymorph. This verifies our assumption regarding the source of the broad peak at 18.3° in the water-cooled material. The third peak at 30.8° corresponds to the [200] and [110] planes of the β phase, while the new peaks at 36.6° correspond to the [021] and [020] planes of the α and β phases, respectively. This type of peak shift associated with β-phase formation has also been observed elsewhere.[13,14] The middle peak profile shows the result of very high draw ratio. Here, due to very high c-axis orientation, higher angle peaks corresponding to [ijk] planes with k non-zero, do not appear in the flat face in measurable quantity. Furthermore, there are only two major peaks in this profile, that at 18.4°, due to the [020] plane of the α polymorph, and that at 20.7°, corresponding to the [200] and [110] planes of the β polymorph. The [100] peak of the α phase, seen at draw ratio of 15, has also reduced to a very small shoulder. This trend of disappearance of the [100] peak of the α phase as the draw ratio is increased has also been observed elsewhere.[13,14]

Figure 8 shows x-ray scans taken along the c direction of the films shown in Figure 7. The lower plot for the water-cooled, undrawn film shows a very broad peak corresponding to the presence of the [100], [020], and [110] planes of the α phase. The second broad peak appearing at 26.5° corresponds to the [021] plane and the peak at 38.8° corresponds to the [131] plane, which is seen to be much larger in this direction (i.e., extrusion direction) compared to the flat-face direction. This further verifies the ability of our die flow to produce c-axis-orientation. As the draw ratio increases to about 15, the magnitude of

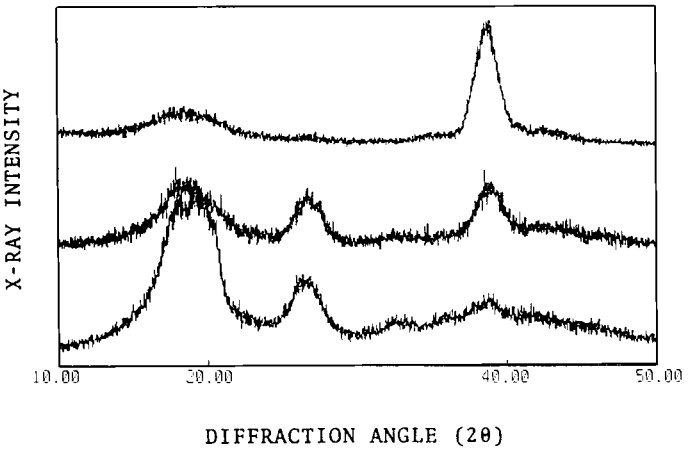

Fig. 8. C-direction x-ray diffraction patterns of extruded films. q = 0.016 cm^2/s; T = 200°C. Top: draw ratio = 85; middle: draw ratio = 15; bottom: water cooled.

the first peak (i.e., the a–b peaks) is greatly reduced (more c-axis orientation) while the magnitude of the third peak appearing at 40.8°, corresponding to [201] and [111] planes of the β polymorph, is greatly enhanced. This trend is further verified by our high draw ratio material where the a–b peaks have essentially completely disappeared and a single peak at 41° ([201] and [111] of the β polymorph) is observed corresponding to an almost perfectly c-axis oriented material (top profile). The rocking curve of the 40° peaks for the drawn films showed half angles of 7 and 15 degrees, respectively, at draw ratios of 85 and 15 indicating c-axis orientation is distributed in a cone with a half angle of 7° in the case of the highly drawn film and 15° in the case of the intermediate drawn film. In general, the rocking curve experiments showed a range of 7° (draw ratio = 85) to 20° (draw ratio = 10) for the half angle.

Finally, with regard to the tensile properties, Figure 9 shows that for draw ratios in the range of 15–85, moduli ranged from ~ 4 to 6.5 GPa. Further-

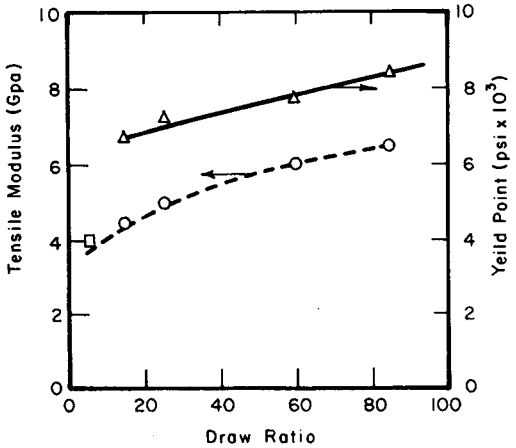

Fig. 9. Tensile modulus and yield point as a function of draw ratio.

more, the yield point also increased from about 6.7×10^3 psi to about 8.3×10^3 psi over the same range.

CONCLUSIONS

Taken together, the results of this study indicate a number of important features regarding the effects of processing history on the morphology and polymorphic phase transformations of PVF_2. We have shown that the extensional flow in our converging channels flow geometry is capable of producing row-nucleated structures at relatively low flow rates, and, from birefringence measurements, we estimate that a minimum extensional stress level in the melt of 1.4×10^6 dyne/cm^2 is needed to induce transformation to the oriented morphology in undrawn quenched samples. Further, such preorientation of the melt by extensional flow enhances the $\alpha \rightarrow \beta$ transformation under our draw conditions. The resultant films also exhibited a relatively high degree of crystallinity ($\sim$ 67% for DR $\leq$ 50) and, in consequence of the high orientation, improved mechanical properties. In summary, the polymorphic transitions under our processing conditions can be listed as follows:

1. Unoriented α to oriented, superheatable α for all extrusion temperatures and DR $\leq$ 5;
2. Increased α to β transformation for 5 < DR $\leq$ 25 and T < 130°C resulting in coexistence of both phases in the resultant film;
3. Transformation of amorphous material to oriented α phase and increased orientation of the coexisting β phase for DR > 25.

This study has been carried out under a grant from the National Science Foundation, MSM 8418643 for which the authors wish to express their gratitude. We would also like to thank Professor P. H. Geil of the Polymer Group, Materials Science and Engineering Department, for help in obtaining and interpreting our electron micrographs.

References

1. H. Kawai, *Jpn. J. Appl. Phys.*, **8**, 975 (1969).
2. J. G. Bergman, J. H. McFee, and G. R. Grane, *Appl. Phys. Lett.*, **18**, 203 (1971).
3. A. J. Lovinger, *Macromolecules*, **15**, 40 (1982).
4. M. A. Bachmann and J. B. Lando, *Macromolecules*, **14**, 40 (1981).
5. R. Hasegawa, Y. Takahashi, Y. Chatani, and H. Tadokoro, *Polym. J.*, **3**, 600 (1972).
6. R. Hasegawa, M. Kobayashi, and H. Tadokoro, *Polym. J.*, **3**, 591 (1972).
7. A. J. Lovinger, *Polymer*, **22**, 412 (1981).
8. Ye. L. Gal'perin, Yu. V. Strogalin, and M. P. Mlenik, *Vysokomol. Soyed.*, **7**, 933 (1965) [Translated in *Polym. Sci. U.S.S.R.*, **7**, 1031 (1965)].
9. J. B. Lando, H. G. Olf, and A. Peterlin, *J. Polym. Sci. A-1*, **4**, 941 (1966).
10. A. J. Lovinger, *Macromolecules*, **14**, 322 (1981).
11. M. Bachmann, W. L. Gordon, S. Weinhold, and J. B. Lando, *J. Appl. Phys.*, **51**, 5095 (1980).
12. A. J. Lovinger, in *Developments in Crystalline Polymers-1*, D. C. Bassett, Ed., Applied Science, London, 1982, Chap. 5.
13. B. P. Kosmynin, Ye. L. Gal'perin, and D. Ya. Tsvankin, *Vysokomol. Soyed.*, **12**, 1254 (1970) [Translated in *Polym. Sci. U.S.S.R.*, **12**, 1418 (1970)].
14. K. Matsushige, K. Nagata, S. Imada, and T. Takemura, *Polymer*, **21**, 1391 (1980).
15. J. C. McGrath and I. M. Ward, *Polymer*, **21**, 855 (1980).
16. A. Richardson, P. S. Hope, and I. M. Ward, *J. Polym. Sci., Polym. Phys. Ed.*, **21**, 2525 (1983).

17. D. C. Yang and E. L. Thomas, *J. Mat. Sci., Lett.*, **3**, 929 (1984).
18. T. C. Hsu, Ph.D. thesis, University of Illinois, Urbana, 1987.
19. T. Shimada, A. E. Zachariades, W. T. Mead, and R. S. Porter, *J. Cryst. Growth*, **48**, 334 (1980).
20. W. T. Mead, A. E. Zachariades, T. Shimada, and R. S. Porter, *Macromolecules*, **12**, 473 (1979).
21. A. G. Kolbeck and D. R. Uhlmann, *J. Polym. Sci. Polym. Phys. Ed.*, **15**, 27 (1977).

Received September 29, 1987
Accepted November 19, 1987